

Evaluation and analysis of radiation exposure to normal tissues during gamma knife radiosurgery for vestibular schwannoma

J.A. Lee^{1,2}, S.R. Kim¹, S.H. Yoon¹, J.S. Kim¹, H.J. Yang^{1*}, G.H. Kim³

¹Department of Bio-medical Science, Korea University, Sejong 30019, Korea

²Department of Radiation Oncology, The Catholic University of Korea Incheon St. Mary's Hospital, Incheon 21431, Korea

³Yonsei University Health System, Severance Hospital Yonsei Gamma Knife Center, Seoul 03788, Korea

ABSTRACT

► Original article

*Corresponding author:

Hyung Jin Yang, Ph.D.,

E-mail: yangh@korea.ac.kr

Received: May 2021

Final revised: October 2021

Accepted: October 2021

Int. J. Radiat. Res., July 2022;
20(3): 571-578

DOI: 10.52547/ijrr.20.3.8

Keywords: Gamma knife radiosurgery, secondary radiation exposure, secondary cancer, Vestibular schwannoma.

Background: A follow-up study of gamma knife radiosurgery has shown that postoperative radiation necrosis, radiation-induced edema, and malignant metastasis may occur. This may be due to secondary radiation exposure, therefore, it becomes necessary to actively reduce exposure to normal organs. **Materials and Methods:** In this study, the secondary radiation dose to the surrounding normal organs was measured during gamma-knife radiosurgery for vestibular schwannoma disease. Using a human pediatric phantom and a glass dosimeter, a treatment plan was established according to the tumor volume, and then the exposure dose to important normal organs in both eyes, thyroid gland, sternum, and both lungs was measured. **Results:** According to this study, the cancer occurrence probability due to secondary exposure was calculated to be 7 cases per 100,000 people up to the case of the eye and thyroid gland. Exposure doses of 100.2 ± 0.79 mGy or more were measured in both eyes, which is approximately 1000 times that of a chest X-ray or a flight from Seoul to New York. This indicates exposure through gamma knife surgery. The dose to the thyroid gland was 12.7 ± 0.05 mGy, which exceeds the effective dose of 10 mSv in abdominal computed tomography. **Conclusion:** By measuring the secondary exposure dose to normal organs during gamma-knife surgery for vestibular schwannoma disease, it was confirmed that the eyes and thyroid gland were exposed dangerously. Therefore, for pediatric patients specifically, a treatment plan that actively reduces secondary exposure is required.

INTRODUCTION

During radiation surgery, the patient is susceptible to radiation exposure to surrounding normal organs or tissues ⁽¹⁾. In radiation surgery, the treatment planning stage goal is to increase tumor control probability and reduce side effects in normal tissues ⁽²⁻³⁾. However, with the recent increase in patients receiving radiation therapy, several cases of secondary tumors have been reported, including radiation therapy using relatively low doses ⁽⁴⁾. Tumors associated with radiation therapy and surgery typically occur in proportion to the radiation dose to which children are more susceptible ⁽⁵⁾. Although medical exposure directly benefits patients, managing patient exposure based on the principle of justification and optimization without applying dose limits has been emphasized. It is important to manage radiation dosage to avoid undesirable biological effects ⁽⁶⁾. Kourinou *et al.* reported that the

incidence of breast, thyroid, and lung cancers due to exposure to peripheral doses after treatment for brain tumors, acute leukemia, and Hodgkin's disease in the neck was 1186 per 1,000,000 patients ⁽⁷⁾. Athar *et al.* reported that children under 58 years undergoing proton radiation therapy for brain tumors suffered from a secondary risk of developing thyroid cancer ⁽⁸⁾. Nazemi-Gelyan *et al.* measured the doses absorbed by the teeth, lens, and optic nerves during radiation therapy for brain tumors using thermo luminescent dosimeters ⁽⁹⁾. Hasegawa evaluated the quality of life of patients ten years post radiosurgery for vestibular schwannomas. Based on a retrospective cohort study, balance issues, headaches, and facial nerve dysfunction occurred after surgery ⁽¹⁰⁾. Ionizing radiation provides sufficient energy to change the structure of molecules in human cells, including DNA ⁽¹¹⁾. Some of these molecular changes are extremely complex, rendering it difficult for the human body to repair them effectively. Evidence suggests that a

small fraction of these changes results in cancer or other health effects.

Radiation surgery using a gamma knife (GK) was developed by Lars Leksell to treat patients with functional disorders ⁽¹²⁾. As GK radiation surgery involves exposure to large doses of radiation at a single instance, the dose delivered to surrounding normal organs can be significant and dangerous ⁽¹³⁾. GK radiation surgery is less invasive than surgical treatment and is used to treat lesions located deep in the brain or in functionally critical areas. Its treatment range has expanded to include benign and malignant brain tumors and arteriovenous malformations. Vestibular schwannoma patients are treated with GK surgery worldwide, and treatment planning for this procedure is developed using computed tomography (CT) and magnetic resonance imaging (MRI). GK radiation surgery involves the destruction of cancer cells by a single, high-energy radiation dose ⁽¹⁴⁾. Therefore, concerns regarding the side effects of acute exposure have been raised ⁽¹⁵⁾.

Sensitivity to radiation exposure differs depending on the organ. In particular, the eye lens is most sensitive to radiation, and radiation exposure to the eye lens leads to cataracts and lens clouding. According to the 2007 recommendations of the International Commission on Radiological Protection, when essential blood vessels or connective tissues of the lens are damaged, the effects of this damage may occur months or years after exposure ⁽¹⁶⁾. More than one radiation surgery is required to treat brain tumors, as supported by clinical experience and studies pertaining to the re-irradiation of brain tumors at metastases ⁽¹⁷⁾. In other words, secondary radiation exposure to the eye lens, which is a sensitive organ, should be emphasized when planning radiation surgeries. Furthermore, according to ICRP Publication 135, lens exposure should be monitored closely during imaging tests such as skull radiography ⁽¹⁸⁾.

According to Chun's study on complications after 5 years of follow-up after gamma knife radiosurgery, 10 out of 17 patients developed radiation necrosis with cysts, radiation-induced edema, and malignant metastasis ⁽¹⁹⁾. Therefore, the most important consideration should be given to the prevention of radiation exposure to normal organs. For benign glioma patients, a radiosurgery plan of 18.2 Gy, the same average dose as in our study, was established.

Paddick *et al.*, who studied the risk of normal organ radiation exposure, suggested that children aged 5 to 15 years and young adults should be careful during radiosurgery. In this study, the peripheral doses at 18, 43, and 70 cm away from the tumor location were calculated using the RadRAT calculator ⁽²⁰⁾. In our study, vestibular schwannoma disease, an average dose of 13 Gy was irradiated, and 18 cm away from the target it was 9.3 mGy (similar to 12 mGy for our study of thyroid), and 43 cm away was 2.0 mGy

(in our study of both lungs 3.3 mGy) and 0.4 mGy was measured at a distance of 70 cm.

This study aimed to measure and analyze the secondary exposure dose delivered to critical organs during GK radiosurgery. We set the tumor volume to four areas during radiosurgery for vestibular schwannoma disease and quantitatively measured the dose to surrounding normal organs using a glass dosimeter.

Quantitative measurements of the doses absorbed by both eyes, thyroid, sternum, and both lungs were evaluated using a pediatric phantom. The average and standard deviation of the measured doses for six normal organs were evaluated using the Kruskal-Wallis test.

MATERIALS AND METHODS

Gamma knife (GK) radiosurgery is used to treat functional brain diseases such as neuralgia, chronic pain, and movement disorders, as well as primary and metastatic malignant brain tumors.

Major equipment

The GK in this study was based on the sixth-generation ICON™ model (Elekta Instruments AB, Stockholm, Sweden), which is the latest model capable of split-irradiation using cone beam CT.

Image-guided radiation surgery is advantageous because it can be performed using a face mask instead of a stereotactic frame, which is used in stereotactic radiosurgery; therefore, screw fixation for affixing the patient's head is avoided making it painless.

Computed Tomography Image acquisition

In this study, images with a 1 mm slice thickness were acquired using a GE Light-Speed Radiation Therapy CT simulator (GE Healthcare, Chicago, IL, USA) for radiosurgery planning.

Radiosurgery plan

To set the virtual tumor volume for the experiment, 480 vestibular schwannoma patients were analyzed from January 2015 to March 2020, and the tumor volumes (from minimum to maximum) were recorded.

A contour of the tumor in the human phantom was depicted based on a mean dose of 18.2 ± 3.3 Gy at a volume of 0.251 cm^3 , 18.4 ± 3.3 Gy at a volume of 0.506 cm^3 , 18.9 ± 3.3 Gy at a volume of 1.008 cm^3 , and 18.4 ± 3.4 Gy at a volume of 2.032 cm^3 . A total of four vestibular schwannoma tumor volumes were set at 18.5 ± 3.4 Gy. Virtual tumor volumes were classified into four categories (figure 1).

Radiosurgery process

The image was transmitted through DICOM (Digital Imaging and Communications in Medicine)

and the irradiation dose was calculated using a Leksell Gamma Plan™ (Elekta Instruments AB, Stockholm, Sweden) computer (Version 5.34). The radiation surgery treatment planning stage for vestibular schwannoma was based on dose

calculations using a Leksell gamma knife plan equipment (Hewlett Packard C3700 workstation). The dose algorithm TMR10 was used for radiosurgery planning (21).

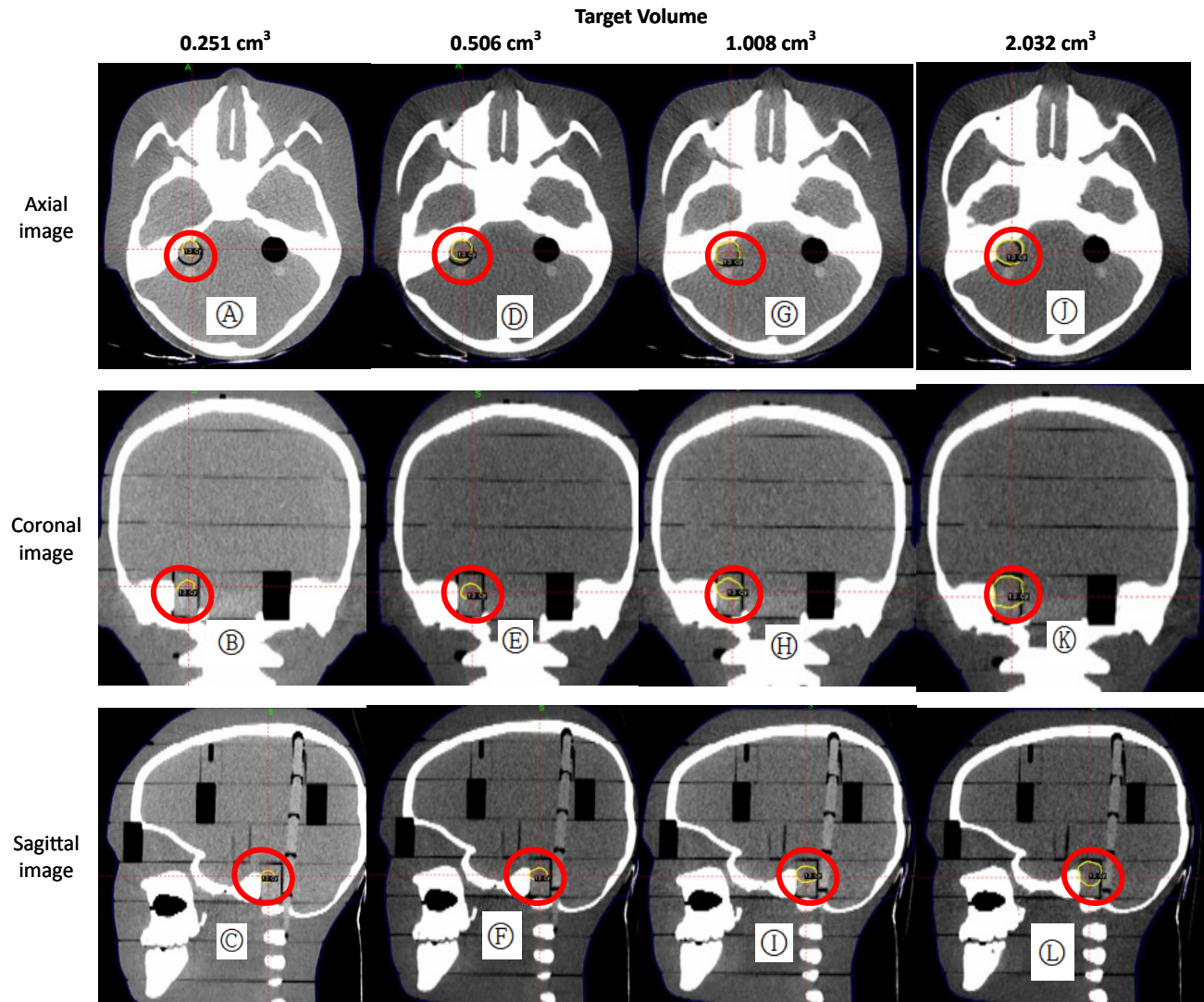


Figure 1. Tumor volume contours (coronary, axial and sagittal images) on the human phantom for radiosurgery planning. Target Volume 0.251 cm³: A, B, C; 0.506 cm³: D, E, F; 1.008 cm³: G, H, I; 2.032 cm³: J, K, L.

Study design

Regarding the region of interest surrounding the brain lesion, six areas were selected: both eyes, thyroid, sternum, and both lungs. Before performing beam irradiation for each volume, the image from the cone beam CT was obtained, and the mean of the error was estimated in the same manner as that in actual radiation surgeries. The brain stem, cochlea, spinal cord, and optic nerve were contoured on the phantom image as critical organs at risk (OARs) during GK radiosurgery planning (table 1). The mean dose delivered to the tumor margin was 13 Gy, and the mean maximal dose was 26 Gy. Similar to real GK surgery, conduction cone beam CT was used to evaluate the phantom setup accuracy prior to performing radiosurgery.

The OARs were compared and analyzed for the

main critical organs of vestibular schwannoma, such as the brain stem, cochlea, spinal cord, and optic nerve (table 1).

Table 1. Exposure doses of four organs at risk during radiosurgery plan (units: Gray).

| Organs at risk | Target Volume | | | |
|----------------|-----------------------|-----------------------|-----------------------|-----------------------|
| | 0.251 cm ³ | 0.506 cm ³ | 1.008 cm ³ | 2.032 cm ³ |
| Brain stem | 0.3 | 1 | 1.3 | 2 |
| Cochlea | 1.2 | 3.4 | 6.5 | 10.7 |
| Spinal cord | 0 | 0 | 0 | 0.1 |
| Optic nerve | 0.2 | 0.4 | 0.2 | 0.4 |

Positional accuracy analysis through cone-beam CT images

After placing the glass dosimeter (GD) on the phantom surface and immediately before the actual beam irradiation, the error values obtained via cone

beam CT were used to verify the exact setup of the position, as shown in table 2. A rotation of 0.5° and a translation of less than 0.6 mm were performed using an accurate phantom and dosimeter setup. In clinical practice, radiation surgery for brain tumors is based on the error limits of 1° and 1 mm. GD was used to measure the dose. It was square shaped and had dimensions of $30\text{mm} \times 40\text{mm} \times 9\text{mm}$.

Table 2. Analysis of position accuracy and three-dimensional error through cone beam computed tomography images before radiation surgery.

| Error | Tumor Volume | Three-dimensional error | | |
|----------------------------|-----------------------|-------------------------|----------------|----------------|
| | | X direction | Y direction | Z direction |
| Rotation error($^\circ$) | 0.251 cm ³ | 0.00 $^\circ$ | 0.02 $^\circ$ | 0.01 $^\circ$ |
| | 0.506 cm ³ | 0.11 $^\circ$ | -0.08 $^\circ$ | 0.06 $^\circ$ |
| | 1.008 cm ³ | -0.03 $^\circ$ | 0.01 $^\circ$ | 0.03 $^\circ$ |
| | 2.032 cm ³ | -0.01 $^\circ$ | 0.34 $^\circ$ | -0.34 $^\circ$ |
| Translation error (mm) | 0.251 cm ³ | 0.00 mm | 0.02 mm | 0.02 mm |
| | 0.506 cm ³ | -0.10 mm | -0.01 mm | 0.04 mm |
| | 1.008 cm ³ | -0.01 mm | 0.01 mm | 0.01 mm |
| | 2.032 cm ³ | 0.58 mm | 0.20 mm | -0.03 mm |

GD calibration

GDs have low direction dependence, and unlike the Thermo Luminescence Dosimeter, they perform measurements using a laser instead of heat; therefore, the measured value does not disappear with a single reading, and it can be read repeatedly. In addition, GDs are highly advantageous as they barely cause degeneration and are not affected by temperature changes in the surrounding environment.

The GD used in this experiment had a measurement range of 1-10 Gy. FGD-202 (AGC Techno Glass Co., Ltd., Japan) was used as the reading device for the GD. A reading system (Fluorescent GD System, Model: FGD_1000SC, Asahi Techno Glass Co., Japan) was used to read the dosage. To achieve better measurement accuracy prior to the experiment, the GD element used in the experiment was subjected to heat treatment (400°C , 1 h) using NEW-3C (Hayashi Denko Co., Ltd., Japan) to remove the residual dose. For dose reading, the average value was obtained after performing the same reading process five times.

Rando phantom irradiation

The phantom used in the experiment was a human body phantom (anthropomorphic phantom: CIRS, Norfolk, VA, Model 706-D) (figure 2) of a 10 years old, composed of a human-tissue-equivalent material; its height was 140 cm, weight was 32 kg, and chest diameter was $17\text{ cm} \times 20\text{ cm}$. It was a cross-sectional dose measurement phantom of a human body model, designed to measure the dose and effective dose delivered to the entire body in the diagnosis area and during radiotherapy by using various dosimeters. The cross-section of the phantom was composed of an extremely flat and smooth tissue-equivalent material, and the phantom was optimized for 22 internal organs with the same structure as the

human body. In addition, all the bones in the phantom were homogeneous and were formulated to represent the average bone tissue based on age. Each cross section comprised a 5-mm-diameter hole, allowing the insertion of a photostimulatory light-emitting dosing device. After heat treatment at 70°C for 30 min to form a uniform color at the center, the readings were obtained. The GDs were placed on the phantom at six locations, and the mean and standard deviation of the measured doses were calculated based on five readings.

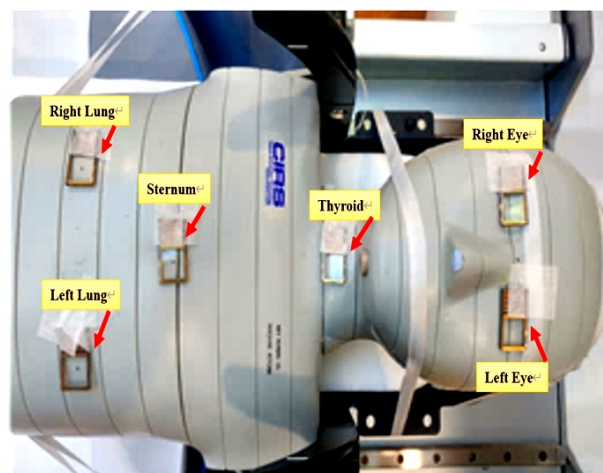


Figure 2. Placement of GD over the areas the measurement for radiation exposure.

Dose unit conversion

The radiation weighting factor (WR) is a dimensionless constant that accounts for the relative biological effectiveness (RBE) of various types of ionizing radiation. The radiation weighting factor is used to calculate the equivalent dose (HT). The equivalent dose is the product of the absorbed dose and the radiation weighting factor. The International Commission on Radiological Protection (ICRP) has published the latest set of numerical values of radiation weighting factor photons as 1⁽²²⁾. Therefore, the absorbed and effective doses shown in our study had the same value.

Calculation of the probability of carcinogenesis

The 'nominal risk factor' was used to calculate the probability of carcinogenesis using the measured radiation dose (Sv). According to ICRP Publication 103, the nominal risk coefficient for radiation is 5.7% per Sv for the entire population. The weighting factor for thyroid tissue was 0.04 and that for lung tissue was 0.12, which was calculated as the average dose to both lungs⁽¹⁶⁾. The probability of carcinogenesis was calculated using equation 1;

Probability of carcinogenesis due to secondary radiation exposure = (Secondary exposure dose) \times (weighting factor) \times 0.057 /Sv (normal risk coefficient) (1)

In this study, the probability of carcinogenesis owing secondary radiation exposure of the thyroid and lungs for a volume of 2.032 cm³ was calculated using equation 2;

Probability of carcinogenesis due to secondary radiation exposure of the thyroid gland and lungs = [0.01265 Sv (thyroid absorbed dose) × 0.04 (thyroid weighting factor) + {0.00342 Sv (right lung absorbed dose) + 0.00333 Sv (left lung absorbed dose)} × 0.12 (lung weighting factor)] × 5.7 × 10⁻² /Sv (normal risk coefficient) = 7.498 × 10⁻⁵ (2)

Statistical analysis

The results were statistically analyzed with the help of SPSS software version 23.0 (SPSS, Chicago, IL). The average and standard deviation of the measured doses for six normal organs were evaluated using the Kruskal-Wallis test. Statistical significance was set at $p < 0.05$.

RESULTS

By analyzing the coordinates of rotation and translation based on the target volume for each case in the x, y, and z axes and in a 3D space, it was determined that the error increased with the tumor volume during both rotation and translation. However, the errors remained below the suggested range ($\pm 3\%$) during the process. (table 2)

Using the GDs placed on normal organs of the phantom, the exposure doses of the normal organs measured at a tumor volume of 0.251 cm³, 0.506 cm³, 1.008 cm³ and 2.032 cm³. Among the virtual tumor volume sizes, the measurement result value of 2.032 cm³, which has the largest volume, is as follows: They were 110.4±0.79 mGy in the right eye, 100.2±1.04 mGy in the left eye, 12.6±0.05 mGy in the thyroid gland, 5.3±0.01 mGy in the sternum, 3.4±0.03 mGy in the right lung, and 3.3±0.02 mGy in the left lung. The right eye (110.4 mGy) was exposed to the highest dose for a target volume of 2.032 cm³.

The dosimetric values for different volume sizes are shown in table 3. For a 2.032 cm³ volume tumor, when irradiating a dose of 18.4 ± 3.4 Gy, the measured exposure dose values for the right and left eyes were 110.4 and 100.2 mGy, respectively. It exceeded 100 mGy per year, which is the threshold dose for lens clouding.

For the target tumor with a volume of 1.008 cm³ and mean irradiation of 18.9 ± 3.3 Gy, an exposure of 10.2 mGy was noted for the thyroid gland. For the vestibular schwannoma subjected to a mean irradiation dose of 18.4 ± 3.4 Gy at a volume of 2.032 cm³, an exposure of 12.7 mGy was noted for the thyroid gland. These values exceed the effective dose of 10 mGy delivered during a CT scan of the abdomen.

The estimated probabilities of carcinogenesis are

summarized in table 4.

The probability of cancer due to radiation exposure to surrounding normal tissues during GK radiation surgery for a tumor volume of 2.032 cm³ refers to the probability that 7 per 100,000 people will develop cancer.

Table 3. Average and standard deviation of measured doses for six normal organs (units: mGy).

| Normal Organs | Target Volume | | | | p value |
|---------------|-----------------------|-----------------------|-----------------------|-----------------------|---------|
| | 0.251 cm ³ | 0.506 cm ³ | 1.008 cm ³ | 2.032 cm ³ | |
| Right Eye | 74.4±0.32 | 88.6±0.53 | 99.0±0.63 | 110.4±0.79 | .000* |
| Left Eye | 33.1±0.47 | 61.7±0.5 | 96.7±0.19 | 100.2±1.04 | .000* |
| Thyroid | 4.2±0.02 | 6.1±0.03 | 10.2±0.04 | 12.6±0.05 | .000* |
| Sternum | 1.9±0.02 | 2.5±0.01 | 3.7±0.01 | 5.3±0.01 | .000* |
| Right Lung | 1.6±0.01 | 1.6±0.01 | 2.6±0.01 | 3.4±0.03 | .001* |
| Left Lung | 1.2±0.00 | 1.2±0.00 | 2.6±0.01 | 3.3±0.02 | .001* |

*p value <.05(Kruskal-Wallis test)

Table 4. The probability of carcinogenesis due to secondary radiation exposure of the thyroid and lungs. The numbers in parenthesis represent the estimated number of occurrences per 100,000 people.

| Probability of carcinogenesis | Target Volume | | | |
|-------------------------------|---------------------------------|---------------------------------|---------------------------------|---------------------------------|
| | 0.251 cm ³ | 0.506 cm ³ | 1.008 cm ³ | 2.032 cm ³ |
| Thyroid | 0.957×10 ⁻⁵ , (1) | 1.390×10 ⁻⁵ , (1) | 2.325×10 ⁻⁵ , (2) | 2.824×10 ⁻⁵ , (3) |
| Right lung | 1.090×10 ⁻⁵ , (1) | 1.094×10 ⁻⁵ , (1) | 1.778×10 ⁻⁵ , (2) | 2.325×10 ⁻⁵ , (2) |
| Left lung | 0.820×10 ⁻⁵ , (1) | 0.820×10 ⁻⁵ , (1) | 1.778×10 ⁻⁵ , (2) | 2.257×10 ⁻⁵ , (2) |
| Thyroid and both lungs | 2.870×10 ⁻⁵ , (3) | 3.306×10 ⁻⁵ , (3) | 5.882×10 ⁻⁵ , (6) | 7.498×10 ⁻⁵ , (7) |

DISCUSSION

According to Ha's study, the current exposure control standard for the general public, 1 mSv per year, is a dose that can cause additional cancer patients with a probability of 1/10–1/10⁵ based on the LNT model (23). In our study, more than 1 mSv was measured in all the results according to the four volumes. Since radiosurgery is performed on patients with brain tumors, it is necessary to be more careful about the possibility of this additional cancer. Also, per Ha's study, when radiation of 100 mSv or more was exposed, abnormal blood test findings appeared within minutes. In our study, the maximum dose to both eyes was measured at 100.2 mGy or more, indicating that abnormal blood test findings can appear immediately due to one gamma knife radiosurgery.

According to a study by Carinou *et al.*, the maximum annual eye exposure dose for medical physicists working in interventional radiology was 15mSv or more. This dose value is considered to be thoroughly monitored for eye exposure dose in accordance with the professional guidelines of the regulatory authorities. However, our study results indicate a maximum of 100.2 mSv was measured in both eyes and the exposure dose was more than 6 times higher than that of Carinou, *et al.* Therefore, it

is necessary to carefully consider the exposure dose to the eye ⁽²⁴⁾.

For a 2.032 cm³ volume tumor, when irradiating a dose of 18.4±3.4 Gy, the measured exposure dose values for the right and left eyes were 110.4 and 100.2 mGy (table 3), respectively. It exceeded 100 mGy per year, which is the threshold dose for lens clouding ⁽²⁵⁾. This value is approximately 1000 times the radiation dose exposure during a chest X-ray scan or a Tokyo–New York flight. Cataracts are known to occur after prolonged exposure to doses exceeding 0.15 Gy/y.

The results of our study showed that the dose exceeded 100 mSv, the threshold dose for lens opacity, in the left eye, even though it was set as right vestibular schwannoma disease and the tumor location was contoured to the right.

The National Council on Radiation Protection and Measurements reported that radiation-induced ocular lens damage includes loss of transparency or blurred vision several years after radiation exposure ⁽²⁶⁾. This suggests that lens damage may occur at lower doses than previously considered and that it would be wise to reduce the dose limit of the lens to 50 mGy. In the experiment, the measured radiation dose delivered to the right eye exceeded 70 mGy, i.e., 74.4 mGy, even for the smallest volume of 0.251 cm³.

Elmtalab *et al.* studied the incidence of secondary thyroid cancer in 3D-conformal radiotherapy and intensity-modulated radiotherapy for high-grade gliomas ⁽²⁷⁾. The excess relative risk (ERR) study showed that the ERR of the thyroid gland increased by 27.7% from 60s to 20s in the adult age group. For children, this ERR is expected to increase further.

According to a study by Iglesias *et al.*, the thyroid gland is sensitive to radiation exposure since radiation increases the risk of thyroid cancer for an average exposure exceeding 50 mGy or after an incubation period of 5–10 years post radiation exposure ⁽²⁸⁾. In particular, it was suggested that patients exposed to external radiation before the age of 4 years had a five times higher risk of developing thyroid cancer per Gy compared to those aged 10–14 years. All risks are predicted to increase significantly when the child is younger. Iglesias *et al.* suggested the importance of radiographic examination for minimization, suggesting that the maximum CT scan dose for young children is 10 mSv. In our study, the thyroid dose was 10.2 mGy for a tumor of 1.008 cm³ and 12.6 mGy for a tumor of 2.032 cm³, resulting in exposure doses exceeding 10 mGy.

In our measurements, the radiation dose of the thyroid for a target volume of 2.032 cm³ was 12.6 mGy, which is lower than the reference value mentioned above. This is because vestibular schwannomas are located far from the thyroid. However, considering that thyroid cancer may occur 50 years post radiation exposure, exposure to critical organs, including the thyroid, should be emphasized.

Radiation exposure can cause breast cancer, leukemia, and thyroid cancer ⁽²⁹⁾.

The effective dose for one CT scan of the abdomen is 10 mSv. The target volume of 1.008 cm³ considered in this experiment was similar to the measured thyroid dose of 10.2 mGy. The importance of low-dose exposure has been indicated, and many hospitals already use low-dose CT equipment for radiological testing. In addition, with respect to the thyroid gland, which is highly susceptible to radiation carcinogenesis, the maximum exposure for a target volume of 2.032 cm³ was 12.7 mGy. Because of the nature of this experiment, in which the brain was set as the tumor target, the dose may be considered insufficient. However, the thyroid cancer incidence rate was reported to be higher than the natural incidence rate in children exposed to <1 mGy.

According to a study by Taylor *et al.*, the US guidelines for pediatric oncology recommend thyroid screening after five years in girls who had received more than 30 Gy of radiation around the thyroid gland ⁽³⁰⁾.

In our study, an average of 18.5 Gy was irradiated in one radiosurgery. Assuming that another radiographic examination and additional radiotherapy are required, it is considered that the radiation treatment for brain tumors gave enough exposure to be considered for thyroid examination. Taylor's study analyzed 50 people—out of 17,980 5-year survivors diagnosed with cancer under 15 years of age in the U.K. It was found that a total of 4 people died from thyroid cancer. In these children, when the thyroid gland received radiation therapy or when the thyroid gland was exposed to scattered ambient doses (e.g., head and neck, spine, mantle, mediastinum, or total body irradiation), the dose was 1,000 to 4,600 cGy range. Their study is different from our study of 12.6 mGy (based on a target volume of 2.032 cm³) because it includes the dose directly exposed to the thyroid for thyroid cancer. However, even if the thyroid is not directly exposed to radiation, it can be seen that the thyroid is a vulnerable organ even with the radiation dose due to scattered radiation.

The study of Rampinelli *et al.* analyzed the risk of lung cancer caused by radiation exposure to computed tomography ⁽³¹⁾. It showed a cancer rate of 0.05% over a 10-year period for those over 50 years old, which corresponds to about 2.4 cases out of a total of 5203 cases. The median cumulative effective dose was 9.3 mSv for men and 13.0 mSv for women. In our study, a single irradiation of brain radiosurgery resulted in a maximum dose of 19.3 mGy to the lungs and thyroid. Even for their study examined with low-dose CT and the cumulative effective dose over a 10-year period, it suggests that attention should be paid to the exposure dose to normal organs due to radiosurgery.

In our experiment, the radiation dose in the right

lung for a target volume of 0.251 cm³ was 1.6 mGy, which is a significant exposure because mammography is limited to once per year. The effective dose for one abdominal CT scan was 10 mSv. The exposure to the thyroid was 10.19 mGy for a target volume of 1.008 cm³.

In our study, doses to the sternum, left lung, and right lung were measured as exposure doses to normal organs. Both lungs produced relatively low doses compared to the other organs. However, by contouring the tumor on the right side, higher exposure dose values were measured in the right lung than in the left. Since the sternum and both lungs are organs that are far from the target, according to our study results, the risk of gamma knife radiosurgery is low.

In our measurements, a dose of 1.6±0.01 mGy to the right lung with a tumor volume of 0.251 cm³ is comparable to a single mammogram dose. Compared with the patient dose value during radiographic examination, the effective dose value for mammography was 1.2 mGy.

The limitations of this study include the inability to measure doses by placing a dosimeter at a point corresponding to the position of the internal organ in the phantom. More meaningful results can be derived if future studies are performed by supplementing the limitations of the study. Repeated radiotherapy can cause cancer metastasis, not only in primary cancer but also in the surrounding and other areas ⁽³²⁾. In particular, the right eye and thyroid were exposed to large doses; therefore, radiation surgery must be planned carefully. Regarding vestibular schwannomas, each volume-dependent GD was used to measure the dose and risk of normal critical organs around the brain.

As shown in this experiment, it is necessary to emphasize the risk of secondary radiation exposure to important normal tissues in the brain during radiation surgery for vestibular schwannomas (table 3, figure 3). In particular, the cochlea was subjected to a maximum dose of 10.7 Gy; as it is an important organ for detecting sound, it must be emphasized more than other organs when planning radiosurgery.

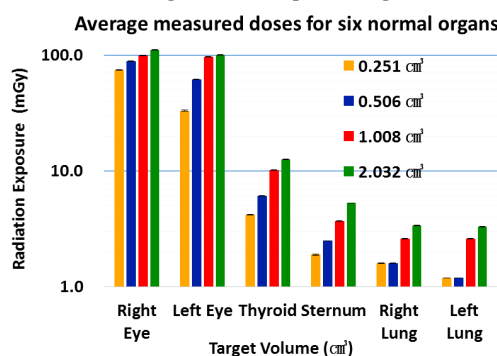


Figure 3. Average measured doses and their standard deviations for six normal organs; Dose measurement was performed a total of 5 times to calculate the average dose value. Error bars indicate the standard deviation of the measurement values performed 5 times. (Radiation scale is represented in log scale).

CONCLUSION

We measured and analyzed the secondary exposure doses delivered to the right eye, left eye, thyroid, sternum, right lung, and left lung during GK radiosurgery for vestibular schwannomas.

Tumor volumes of 0.251 cm³, 0.506 cm³, 1.008 cm³, and 2.032 cm³ in vestibular schwannoma disease. Four radiosurgery plans were established, and measurements were made with a glass dosimeter using a pediatric human phantom. An analysis of the cancer occurrence rate for the thyroid gland and lungs revealed that 7 out of 100,000 people might develop cancer.

Our study highlights the importance of protecting normal tissues during radiosurgery planning by studying the risk of secondary radiation exposure that may occur during radiosurgery.

ACKNOWLEDGEMENTS

This work was supported by the Research Foundation of Korea University.

Ethical considerations: Not applicable.

Conflict of interest: All authors declare no conflict of interest.

Funding: This study was supported by the Research Foundation of Korea University (K1915361).

Author contributions: All authors contributed equally to the design of the study, data collection and analysis, and the writing of the manuscript. All authors read and approved the final manuscript.

REFERENCES

- Di Betta E, Fariselli L, Bergantin A, Locatelli F, Del Vecchio A, Brogi S, et al. (2010) Evaluation of the peripheral dose in stereotactic radiotherapy and radiosurgery treatments. *Med Phys*, **37**(7): 3587–3594.
- Labby ZE, Barraclough B, Bayliss RA, Besemer AE, Dunkerley DAP and Howard SP (2018) Radiation treatment planning and delivery strategies for a pregnant brain tumor patient. *J Appl Clin Med Phys*, **19**(5): 368–374.
- Choi K and Cho JK (2021) Development and statistical assessment of a radiation safety literacy measurement tool. *Int J Radiat Res*, **19**(1):41–48.
- Cooksey R, Wu SY, Klesse L, Oden JD, Bland RE, Hodges JC, et al. (2019) Metabolic syndrome is a sequela of radiation exposure in hypothalamic obesity among survivors of childhood brain tumors. *J Invest Med*, **67**(2): 295–302.
- Hess CB, Thompson HM, Benedict SH, Seibert JA, Wong K, Vaughan AT, et al. (2016) Exposure risks among children undergoing radiation therapy: considerations in the era of image guided radiation therapy. *Int J Radiat Oncol Biol Phys*, **94**(5): 978–992.
- Wolf A, Naylor K, Tam M, Habibi A, Novotny J, Liščák R, et al. (2019) Risk of radiation-associated intracranial malignancy after stereotactic radiosurgery: a retrospective, multicentre, cohort study. *Lancet Oncol*, **20**(1): 159–164.
- Kourinou KM, Mazonakis M, Lyraraki E, Stratakis J and Damilakis J (2013) Scattered dose to radiosensitive organs and associated risk for cancer development from head and neck radiotherapy in pediatric patients. *Phys Med*, **29**(6): 650–655.
- Athar BS and Paganetti H (2011) Comparison of second cancer risk due to out-of-field doses from 6-MV IMRT and proton therapy based on 6 pediatric patient treatment plans. *Radiother Oncol*,

- 98(1): 87–92.
9. Nazemi-Gelyan H, Hasanzadeh H, Makhdumi Y, Abdollahi S, Akbari F, Varshoe-Tabrizi F, et al (2015) Evaluation of organs at risk's dose in external radiotherapy of brain tumors. *Iran J Cancer Prev*, **8**(1): 47–52.
10. Shinya Y, Hasegawa H, Shin M, Sugiyama T, Kawashima M, Takahashi W, et al (2019) Long-term outcomes of stereotactic radiosurgery for vestibular schwannoma associated with neurofibromatosis type 2 in comparison to sporadic schwannoma. *Cancers*, **11**(10): 1498.
11. O'Connor MK (2017) Risk of low-dose radiation and the BEIR VII report: A critical review of what it does and doesn't say. *Phys Med*, **43**: 153–158.
12. Castinetti F, Brue T, Morange I, Carron R and Régis J (2017) Gamma Knife radiosurgery for hypothalamic hamartoma preserves endocrine functions. *Epilepsia*, **58**(2): 72–76.
13. Zeverino M, Jaccard M, Patin D, Ryckx N, Marguet M, Tuleasca C, et al. (2017) Commissioning of the Leksell gamma Knife® Icon™. *Med Phys*, **44**(2): 355–363.
14. Ei-Shehaby AMN, Reda WA, Abdel Karim KM, Emad Eldin RM and Nabeel AM (2017) Gamma knife radiosurgery for cerebellopontine angle epidermoid tumors. *Surg Neurol Int*, **8**: 258.
15. Modorati GM, Dagan R, Mikkelsen LH, Andreasen S, Ferlito A and Bandello F (2020) Gamma knife radiosurgery for uveal melanoma: a retrospective review of clinical complications in a tertiary referral center. *Ocul Oncol Pathol*, **6**(2): 115–122.
16. ICRP Publication 103, The 2007 Recommendations of the International Commission on Radiological Protection. Publication 103-Annals of the ICRP **37**:(2-4)-Free_extract.pdf
17. Asher AL, Burri SH, Wiggins WF, Kelly RP, Boltes MO, Mehrlich M, et al. (2014) A new treatment paradigm: neoadjuvant radiosurgery before surgical resection of brain metastases with analysis of local tumor recurrence. *Int J Radiat Oncol Biol Phys*, **88**(4): 899–906.
18. ICRP Publication 135, Diagnostic reference levels in medical imaging. ICRP Publication 46, 1 2017,
19. Chun SM, Lim YJ, Leem W, Kim TS, Rhee BA (2001) Gamma knife radiosurgery for low grade glioma - long-term follow-up results. *J Korean Neurosurg Soc*, **30**(2): 273–280.
20. Paddick I, Cameron A, Dimitriadis A (2021) Extracranial dose and the risk of radiation-induced malignancy after intracranial stereotactic radiosurgery: is it time to establish a therapeutic reference level?. *Acta Neurochir (Wien)*, **163**(4): 971–979.
21. Fallows P, Wright G, Harrold N, Bownes P (2018) A comparison of the convolution and TMR10 treatment planning algorithms for Gamma Knife® radiosurgery. *J Radiosurg SBRT*, **5**(2): 157–167.
22. Menzel HG and Harrison J (2012) Effective dose: a radiation protection quantity. *Ann ICRP*, **41**(3-4): 117–123.
23. Ha MN (2011) Radiation Exposure and Cancer. *J Clin Otolaryngol Head Neck Surg*, **22**(2): 275–281.
24. Carinou E, Ginjaume M, O'Connor U, Kopec R and Sans Merce MS (2014) Status of eye lens radiation dose monitoring in European hospitals. *J Radiol Prot*, **34**(4): 729–739.
25. Boal TJ, Pinak M (2015) Dose limits to the lens of the eye: International Basic Safety Standards and related guidance. *Annals of the ICRP*, **44**(1): 112–117.
26. Dauer LT, Ainsbury EA, Dynlacht J, Hoel D, Klein BEK, Mayer D, et al. (2017) Guidance on radiation dose limits for the lens of the eye: overview of the recommendations in NCRP Commentary No. 26. *Int J Radiat Biol*, **93**(10): 1015–1023.
27. Elmtalab S and Abedi I (2021) Investigating the out-of-field doses and estimating the risk of secondary thyroid cancer in high-grade gliomas radiation therapy with modulated intensity and 3D-conformal: a phantom study. *Int J Radiat Res* **19**(3): 569–574.
28. Iglesias ML, Schmidt A, Ghuzlan AA, Lacroix L, Vathaire F, Chevillard S, et al. (2017) Radiation exposure and thyroid cancer: a review. *Arch Endocrinol Metab*, **61**(2): 180–187.
29. Koo E, Henderson MA, Dwyer M, Skandarajah AR, et al. (2020) Radiation-Associated Thyroid Cancer Surveillance and Management in a Cohort of Late Effects Patients. *World J Surg*, **44**: 3028–3035.
30. Taylor AJ, Croft AP, Palace AM, Winter DL, Reulen RC, Stiller CA, Stevens MC, Hawkins MM, et al. (2009) Risk of thyroid cancer in survivors of childhood cancer: Results from the British Childhood Cancer Survivor Study. *Int J Cancer* **125**: 2400–2405.
31. Rampinelli C, Marco P, Origgi D, Maisonneuve P, Casiraghi M, Veronesi G, Spaggiari L, Bellomi M, et al. (2017) Exposure to low dose computed tomography for lung cancer screening and risk of cancer: secondary analysis of trial data and risk-benefit analysis. *The bmj* 356–347.
32. Higuchi Y, Yamamoto M, Serizawa T, Aiyama H, Sato Y and Barford BE (2018) Modern management for brain metastasis patients using stereotactic radiosurgery: literature review and the authors' gamma knife treatment experiences. *Cancer Manag Res*, **10**: 1889–1899.